Luminescence of Erbium Doped Telluride Glass Enhanced by Surface Plasmon of Metallic Silver Nanoparticles

CHEN Xiao-bo[1]，LI Song[1]，ZHAO Guo-ying[2]，LONG Jiang-mi[1]，WANG Shui-feng[1]，ZHENG Dong[1]，WU Zheng-long[1]，MENG Shao-hua[2]，GUO Jing-hua[1]，XU Ling-zhi[2]，YU Chun-lei[3]，HU Li-li[3]

1. Applied Optics Beijing Area Major Laboratory and Physics Department，Beijing Normal University，Beijing 100875，China
2. School of Materials Science and Technology，Shanghai Institute of Technology，Shanghai 200235，China
3. Shanghai Institute of the Optics and Fine Mechanics，Chinese Academy of Sciences，Shanghai 201800，China

Abstract Interesting optical properties of metal surface plasmon，especially the behavior on luminescence enhancement field，have become a hot research topic globally. The surface plasmon is just a kind of collective oscillation made of free electron and light electromagnetic fields because their resonant frequencies are similar when they are interacting with each other. In present paper，the erbium luminescence resonant enhanced by surface plasmon of Ag nanoparticles (NPs) in telluride glass is studied. The absorption，excitation，luminescence spectra，and lifetime are measured. First，we select the 365.5 and 379.0 nm excitation peaks as excitation wavelength to measure the visible luminescence spectra in the wave range of 385～780 nm. We find 4 luminescence peaks positioned at 408.0，525.0，546.0，and 658.5 nm. They are，respectively，the fluorescence transitions of $^2H_{9/2}\rightarrow{}^4I_{15/2}$，$^2H_{11/2}\rightarrow{}^4I_{15/2}$，$^4S_{3/2}\rightarrow{}^4I_{15/2}$，and $^4F_{9/2}\rightarrow{}^4I_{15/2}$ of Er^{3+} ions. It is easy to calculate the peak intensities of the above 4 visible luminescence of (A) Er^{3+}(0.5%)Ag(0.2%)：Telluride glass with the average diameter of 80 nm for Ag NPs are about 1.44～2.52 times larger than that of the (C) Er^{3+}(0.5%)：Telluride glass. Moreover，the peak intensities of the above 4 visible luminescence spectra of (B) Er^{3+}(0.5%)Ag(0.2%)：Telluride glass with the average diameter of 50 nm for Ag NPs are about 1.08～1.55 times larger than that of the sample (C). Then，we select the 365.5 and 379.0 nm excitation peaks as excitation wavelength to measure the near infrared luminescence spectra in the wave range of 928～1 680 nm. It is found that near infrared luminescence peaks are positioned at 979.0 and 1 530.0 nm. They are，respectively，the fluorescence transitions of $^4I_{11/2}\rightarrow{}^4I_{15/2}$ and $^4I_{13/2}\rightarrow{}^4I_{15/2}$ of Er^{3+} ions. The peak intensities of the above 2 near infrared luminescence spectra of sample (A) are about 1.43～2.14 times larger than that of the sample (C). Similarly，the peak intensities of the above 2 near infrared luminescence spectra of sample (B) are about 1.28～1.82 times larger than that of the sample (C). Therefore，the largest enhancement is about 2.52 times larger. From the experiments of fluorescence lifetime dynamics，we find that the 550 nm fluorescence lifetime of sample (A) is about $\tau_A(550)=43.5\ \mu s$，that of sample (B) is about $\tau_B(550)=43.2\ \mu s$，and that of sample (C) is about $\tau_C(550)=48.6\ \mu s$. The experimental results illustrate that $\tau_A\approx\tau_B<\tau_C$. This means that the luminescence enhancement of sample (B) relative to sample (C) results from the spontaneous radiation enhancement effect. However，this also means that the luminescence enhancement of sample (A) relative to sample (B) results from the Size r effect，in which the increased of the scattering cross section C_s is much larger than that of the absorption cross section C_a when r is enlarged，because the scattering cross-section C_s are proportional positive ratio to r^6 and the absorption cross-section C_a are proportional positive ratio to r^3. As we

Received：2018-05-19；**accepted**：2018-10-14

Foundation item：The National Natural Science Foundation of China (51472028) and the Fundamental Research Funds for the Central Universities of China (2017TZ01)

Biography：CHEN Xiao-bo，(1963—)，Professor at Beijing Normal University e-mail：xbchen@bnu.edu.cn

know that the scattering cross-section C_s is the reason for the increase of fluorescence, meanwhile the absorption cross-section C_a is the reason for the decease of fluorescence. When r is increase, scattering cross-section C_s is the main part. When luminescent material couples with the metallic surface Plasmon, the energy is transferred quickly to metallic surface Plasmon, and then scattered to the far field. It's beneficial for the enhancement of fluorescence. As a comprehensive result, the fluorescence is enhanced when r is enlarged. It has excellent application prospects in the optogalvanic electricity generation of solar cell and biophysical application other as well as fields.

Keywords Ag nanoparticles; Luminescence enhancement; Surface plasmon; Telluride glass; Er^{3+} ion

中图分类号: O482.3 **文献标识码**: A **DOI**: 10.3964/j.issn.1000-0593(2019)07-2293-06

Introduction

Interesting optical properties of metal surface plasmon, especially the behavior on luminescence enhancement field, have become a hot research topic globally[1]. In 1902, Wood et al. found that the incident light caused an anomalous diffraction phenomenon after it irradiated at the metal grating. This is the earliest discover of the surface plasmon resonant phenomenon. In 1909, Sommerfeld et al. discovered the wave solutions of electromagnetic wave which is localized near the metal surface. In 1941, Fano et al. explained the anomalous diffraction phenomenon of metal grating according to the theory of Sommerfeld. Moreover, they also proposed the concept of surface plasmon wave. In 1957, the work of Ritchie in the area of surface science led to the discovery of surface plasmon more clearly. Surface plasmon is just a kind of collective oscillation made of free electron and light electromagnetic fields because their resonant frequencies are similar when they are interacting with each other. That is, the collective resonance of metal surface free electrons is usually called Surface Plasmon Polariton (SPP). Weber has calculated, under the premise of conservation of energy, to find that the electric field has been enhanced nearly 100 times because SPP resonance occurs when the silver is excited by the 2.0 eV energy. In the case of sub wavelength and rough (nano) metal surface, the surface plasmon is locality, the electromagnetic field could be enhanced further, with the highest enhancement about 10^7. Lakowicz, Takeho Aisaka, Yan and Yang[2], Okamoto K, Luo and Li[3], He and Zhan[4], Cheng and Jing[5], as well as Song and Yin and Xu[6] et al. have completed a number of excellent works[7-13] with significant enhancement in luminescence. The luminescence of the Er^{3+} ion enhanced by silver nanoparticles in telluride glasses has also been researched[9,12-13]. This has excellent application prospects in the optogalvanic electricity generation of solar cell[7] and biophysical application as well as other fields[8-13].

The region of the local field amplification of the metal surface plasmon is mainly focused on dozens of nanos around the metal. For composite thin film samples, its thickness directly influences the coupling effect between the luminescence center and metal surface plasmon. Therefore, even the luminescence enhancement effect is quite good for most of the work up until nowadays. However, the absolute luminescence intensity is not high. This is the unsolved problem which seriously restricts the application of luminescent materials. We utilize the high-quality telluride luminescence glass to dope silver nanoparticles into its body. Not only is its luminescence enhanced, but its absolute luminescence intensity is also increased to become brighter than in the general case. Moreover, it is achieved by commercial silver nanoparticle, something cheaper and more promising.

1 Instruments, conditions, and the samples

The Telluride glasses were manufactured using highly purified TeO_2, ZnO, La_2O_3, Er_2O_3 and Ag NPs powder as the starting materials. The well-mixed raw materials were placed in the alumina crucible, which were melted at 880 ℃ for 50 min under an oxygen atmosphere. A dry oxygen atmosphere was introduced to remove hydroxyl groups. The melts were then poured into a preheated stainless steel mold and annealed for several hours near the glass transition temperature, T_g (approximately 300 ℃). The annealed samples were cut and polished to a size of 16 mm×20 mm×5.5 mm for optical measurements. The samples used in our experiments were (A) Er^{3+}(0.5%)Ag(0.2%): Telluride glass with the average diameter of 80 nm for Ag nanopartlcles (NPs), (B) Er^{3+}(0.5%)Ag(0.2%): Telluride glass with the average diameter of 50 nm for Ag NPs, and (C) Er^{3+}(0.5%): Telluride glass. The composition of the sample (A), for example, was $70TeO_2$-$25ZnO$-$5La_2O_3$-$0.5Er_2O_3$-0.2Ag NPs in molar based compositions.

The equipment used in our luminescence experiment was FL3-2iHR fluorescence spectrometer (Horiba-JY Co., America, Japan, and France). The excitation light source was a xenon lamp. The visible light detector was an R2658p photomultiplier. The infrared detector was an H10330-75 photo-

multiplier. For all the results, the signal intensities at the same wavelength in the same figure can be compared directly. The absorptions were measured using a UV3600 spectrophotometer (Shimadzu, Japan). The lifetime dynamics were recorded using the same fluorescence spectrometer FL3-2iHR.

2 Results and discussion

2.1 Spectra of absorption and fluorescence

The absorption of the samples (A) and (C) was measured, as is shown in Fig. 1. From Fig. 1, we can find that the absorption of Er^{3+} ion in sample (A) is basically the same as that in sample (C). They are very similar in wave shape, peak intensity, and peak wavelength. The baseline of the absorption of sample (A) is enhanced greatly because of the absorption and scatter of the Ag NPs. It can be found that the absorption line of sample (A) in the range of 1 600～2 500 nm is parallel to that of sample (C), which mainly results from the scatter of the Ag NPs. Meanwhile in the range of 400～1 500 nm, the absorption line of sample (A) emerges a small broad spectral peak position at about 520 nm, which results from the absorption of surface plasmon polariton of the Ag NPs. The phenomenon of that the absorption peak of surface plasmon polariton of the Ag NPs in Telluride glass is small is coincided with the report of references[9,12-13]. Finally, Figure 1 shows that the absorption peaks of Er^{3+} ion in sample (A) are positioned at (1 497.0 nm, 1 531.5 nm), 976.5, 799.0, 652.5, 544.0, 522.0, 489.0, 451.5, 443.5, 406.8, 379.0 and 365.5 nm, respectively. It can be recognized that these absorption peaks are the absorption transitions of $^4I_{15/2}\rightarrow{}^4I_{13/2}$, $^4I_{15/2}\rightarrow{}^4I_{11/2}$, $^4I_{15/2}\rightarrow{}^4I_{9/2}$, $^4I_{15/2}\rightarrow{}^4F_{9/2}$, $^4I_{15/2}\rightarrow{}^4S_{3/2}$, $^4I_{15/2}\rightarrow{}^2H_{11/2}$, $^4I_{15/2}\rightarrow{}^4F_{7/2}$, $^4I_{15/2}\rightarrow{}^4F_{5/2}$, $^4I_{15/2}\rightarrow{}^4F_{3/2}$, $^4I_{15/2}\rightarrow{}^2H_{9/2}$, $^4I_{15/2}\rightarrow{}^4G_{11/2}$, and $^4I_{15/2}\rightarrow{}^4G_{9/2}$ of the Er^{3+} ion[1,10], respectively.

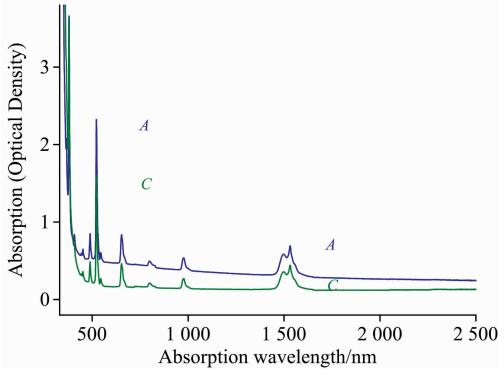

Fig. 1 The absorption of the samples (A) Er^{3+} (0.5%)Ag (0.2%): Telluride glass with 80 nm average diameter for Ag NPs (blue) and (C) Er^{3+} (0.5%): Telluride glass (green)

The excitation spectra of the samples (A), (B) and (C) were measured. First, as is shown in Fig. 2, we select 550.0 nm visible luminescence wavelength as fluorescence measurement wavelength to measure the visible excitation spectra in the wave range of 250.0～508.0 nm. We found 5 excitation peaks positioned au 365.5, 379.0, 406.5, 451.0, and 488.5 nm, respectively. Moreover, we easily recognized that they are the absorption transitions of the $^4I_{15/2}\rightarrow{}^4G_{9/2}$, $^4I_{15/2}\rightarrow{}^4G_{11/2}$, $^4I_{15/2}\rightarrow{}^2H_{9/2}$, $^4I_{15/2}\rightarrow({}^4F_{3/2}, {}^4F_{5/2})$, and $^4I_{15/2}\rightarrow{}^4F_{7/2}$ of the Er^{3+} ion[1,10]. Their peak intensities of the visible excitation spectra 6.83×10^2, 2.42×10^3, 2.90×10^2, 2.59×10^2, 6.73×10^2 for sample (A), and are about 3.69×10^2, 1.85×10^3, 1.82×10^2, 1.70×10^2, 4.74×10^2 for sample (C). For the above mentioned 5 peaks, the intensities of the visible excitation spectra of the sample (A) are 1.85, 1.30, 1.59, 1.52, and 1.42 times larger than that of sample (C), respectively.

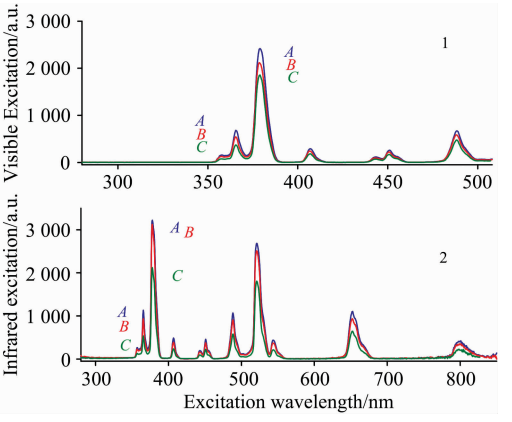

Fig. 2 The visible (1) and infrared (2) excitation spectra of (A) Er^{3+} (0.5%)Ag(0.2%): Telluride glass with the average diameter of 80 nm for Ag NPs (blue), (B) Er^{3+} (0.5%) Ag(0.2%): Telluride glass with the average diameter of 50 nm for Ag NPs (red) and (C) Er^{3+} (0.5%): Telluride glass (green) when being monitored at 550.0 nm (1) and 1 530.0 nm (2) luminescence wavelength

Then, as is also shown in Fig. 2, we select 1 530 nm near infrared luminescence wavelength as fluorescence measurement wavelength to measure the near infrared excitation spectra in the wave range of 250.0～850.0 nm. We found 9 excitation peaks positioned in 365.5, 378.0, 406.5, 451.0, 488.5, 520.5, 543.5, 652.5, and 801.0 nm, respectively. It was recognized that they are the absorption peaks of the $^4I_{15/2}\rightarrow{}^4G_{9/2}$, $^4I_{15/2}\rightarrow{}^4G_{11/2}$, $^4I_{15/2}\rightarrow{}^2H_{9/2}$, $^4I_{15/2}\rightarrow({}^4F_{3/2}, {}^4F_{5/2})$, $^4I_{15/2}\rightarrow{}^4F_{7/2}$, $^4I_{15/2}\rightarrow{}^2H_{11/2}$, $^4I_{15/2}\rightarrow{}^4S_{3/2}$, $^4I_{15/2}\rightarrow{}^4F_{9/2}$, and $^4I_{15/2}\rightarrow{}^4I_{9/2}$ transitions[1,10]. Their peak intensities of the near infrared excitation spectra are about 1.13×10^3, 3.22×10^3, 4.86×10^2, 4.60×10^2, 1.07×10^3, 2.68×10^3, 4.39×10^2, 1.11×10^3, 4.21×10^2 for sample (A), and 5.36

$\times 10^2$, 2.12$\times 10^3$, 2.37$\times 10^2$, 2.25$\times 10^2$, 5.79$\times 10^2$, 1.81$\times 10^3$, 2.13$\times 10^2$, 6.46$\times 10^2$, 2.28$\times 10^2$ for sample (C). For the above mentioned 9 peaks, the intensities of the near infrared excitation spectra of the sample (A) are about 2.12, 1.52, 2.05, 2.05, 1.85, 1.49, 2.06, 1.71, and 1.85 times larger than that of sample (C), respectively.

The luminescence spectra of the samples (A), (B) and (C) were measured. First, as is shown in Figs. 3 and 4, we select the 365.5 and 379.0 nm excitation peaks as excitation wavelength to measure the visible luminescence spectra in the wave range of 385～780 nm. We found 4 luminescence peaks positioned at 408.0, 525.0, 546.0, and 658.5 nm, respectively. They are, respectively, the fluorescence transitions of $^2H_{9/2}\rightarrow{}^4I_{15/2}$, $^2H_{11/2}\rightarrow{}^4I_{15/2}$, $^4S_{3/2}\rightarrow{}^4I_{15/2}$, and $^4F_{9/2}\rightarrow{}^4I_{15/2}$ of Er^{3+} ions[1,10]. Their peak intensities of the visible luminescence spectra are about 2.70$\times 10^0$, 2.56$\times 10^1$, 8.94$\times 10^1$, 7.50$\times 10^{-1}$ for sample (A), 1.57$\times 10^0$, 1.84$\times 10^1$, 5.48$\times 10^1$, 4.85$\times 10^{-1}$ for sample (B), and 1.11$\times 10^0$, 1.43$\times 10^1$, 3.54$\times 10^1$, 3.45$\times 10^{-1}$ for sample (C), when they are excited by the 365.5 nm light. Similarly, their peak intensities of the visible luminescence spectra are about 5.87$\times 10^0$, 1.20$\times 10^2$, 3.67$\times 10^2$, 3.04$\times 10^0$ for sample (A), 3.58$\times 10^0$, 8.99$\times 10^1$, 2.43$\times 10^2$, 2.15$\times 10^0$ for sample (B), and 2.84$\times 10^0$, 8.31$\times 10^1$, 2.04$\times 10^2$, 1.85$\times 10^0$ for sample (C), when they are excited by the 379.0 nm light. It is easy to calculate that the peak intensities of the above 4 visible luminescence of sample (A) are about 1.44～2.52 times larger than that of the sample (C). Moreover, the peak intensities of the above 4 visible luminescence spectra of sample (B) are about 1.08～1.55 times larger than that of the sample (C). In other words, the largest enhancement is about 2.52 times larger for visible luminescence.

Then, as is also shown in Figs. 3 and 4, we select the 365.5 and 379.0 nm excitation peaks as excitation wavelength to measure the near infrared luminescence spectra in the wave range of 928～1 680 nm. It is found that near infrared luminescence peaks are positioned at 979.0 and 1 530.0 nm. They are, respectively, the fluorescence transitions of $^4I_{11/2}\rightarrow{}^4I_{15/2}$ and $^4I_{13/2}\rightarrow{}^4I_{15/2}$ of Er^{3+} ions[1,10]. Their peak intensities of the near infrared luminescence spectra are about 2.84$\times 10^1$, 2.36$\times 10^2$ for sample (A), 2.16$\times 10^1$, 2.01$\times 10^2$ for sample (B), and 1.41$\times 10^1$, 1.10$\times 10^2$ for sample (C), when they are excited by the 365.5 nm light. Similarly, their peak intensities of the near infrared luminescence spectra are about 8.97$\times 10^1$, 7.32$\times 10^2$ for sample (A), 8.04$\times 10^1$, 6.95$\times 10^2$ for sample (B), and 6.28$\times 10^1$, 4.81$\times 10^2$ for sample (C), when they are excited by the 379.0 nm light. The peak intensities of the above 2 near infrared luminescence spectra of sample (A) are about 1.43～2.14 times larger than that of the sample (C). Similarly, the peak intensities of the above 2 near infrared luminescence spectra of sample (B) are about 1.28～1.82 times larger than that of the sample (C). That is, the largest enhancement time is about 2.14 times larger for near infrared luminescence.

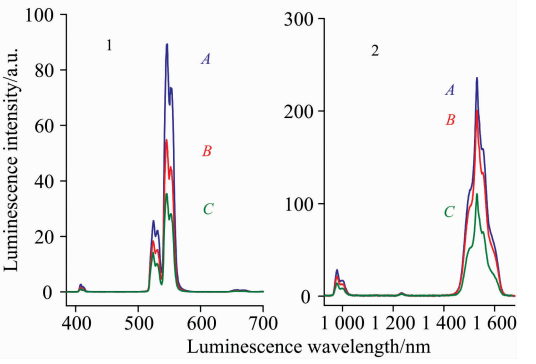

Fig. 3 The visible (1) and infrared (2) luminescence spectra of the samples (A) Er^{3+}(0.5%)Ag(0.2%): Telluride glass with 80 nm average diameter for Ag NPs (blue), (B) Er^{3+}(0.5%)Ag(0.2%): Telluride glass with 50 nm average diameter for Ag NPs (red), and (C) Er^{3+}(0.5%): Telluride glass (green) when excited by 365.5 nm light

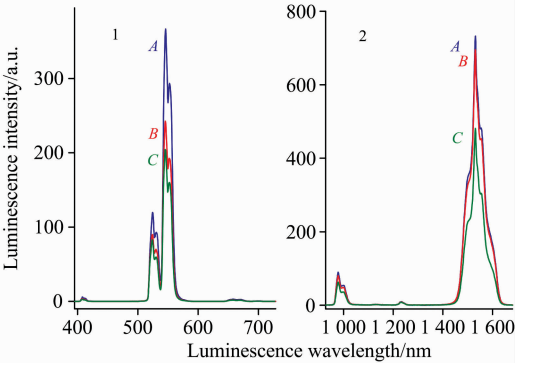

Fig. 4 The visible (1) and infrared (2) luminescence spectra of the samples (A) Er^{3+}(0.5%)Ag(0.2%): Telluride glass with 80 nm average diameter for Ag NPs (blue), (B) Er^{3+}(0.5%)Ag(0.2%): Telluride glass with 50 nm average diameter for Ag NPs (red), and (C) Er^{3+}(0.5%): Telluride glass (green) when excited by 379.0 nm light

2.2 Fluorescence Lifetime Dynamics

The fluorescence lifetime of 550 nm fluorescence of sample (A), (B) and (C) are measured when pulse xenon lamp is used as a pumping source. The measured results are shown in Fig. 5. The 550 nm fluorescence lifetime of sample (A) is about $\tau_A(550)=43.5$ μs, that of sample (B) is about $\tau_B(550)=43.2$ μs, and that of sample (C) is about $\tau_C(550)=48.6$ μs.

2.3 Analysis

The method of introducing nanosilver particles in lumi-

nescence glass is mainly through silver chloride or silver nitrate. In the process of melting glass raw materials, silver chloride or silver nitrate is melted. In the process of subsequent condensation, the silver atoms solidified into nano clusters with the formation of solid glass. Or, the Ag NPs may be obtained by the special heat-treated process. In these ways, nanosilver is generally very small within the few nanometers range, which causes a small number of luminescence enhancements of Er^{3+} ion induced by silver surface Plasmon in luminescence glass. However, we are experimenting with the direct introduction of nanosilver particles that ranges from 10 to more than 100 nm. Because the melting point of silver is 961°. And we control the raw materials of Telluride luminescent glass to be melted at less than 880°. Therefore, the size of the nanoscale particles of Ag will hardly decrease. The most important thing is that we have thus enhanced and controlled the size r of the silver nanoparticles in the Telluride luminescence glass.

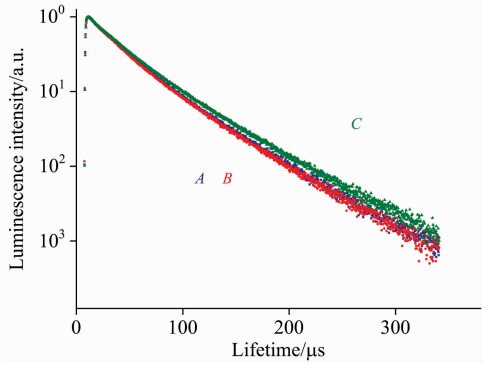

Fig. 5 The fluorescence lifetime of 550 nm fluorescence of (A) Er^{3+} (0.5%) Ag(0.2%): Telluride glass with 80 nm average diameter for Ag NPs (blue), (B) Er^{3+} (0.5%) Ag(0.2%): Telluride glass with 50 nm average diameter for Ag NPs (red), and (C) Er^{3+} (0.5%): Telluride glass (green) when excited by 378 nm pulsed light

According to Mie theory[8], the extinction interface C_e of the spherical metal particles in rough metal surface is about

$$C_e = C_a + C_s \tag{1}$$

The scattering cross section C_s is the reason of fluorescence enhancement, the absorption cross section C_a is the reason of the fluorescence decrease. In which

$$C_s = \frac{k^4}{6\pi} |\alpha|^2 \propto r^6 \tag{2}$$

$$C_a = k \times \mathrm{Im}(\alpha) \propto r^3 \tag{3}$$

$$k = \frac{2\pi n}{\lambda_0} \tag{4}$$

$$\alpha = 4\pi r^3 \left(\frac{\varepsilon_m - \varepsilon}{\varepsilon_m + 2\varepsilon}\right) \tag{5}$$

k is the wave vector of the incident light in the medium, λ_0 is the wavelength of the incident light, n is the refractive index of the medium, α is the polarizability of the sphere when the radius is r, ε_m is the dielectric constant of the metal, ε is the dielectric constant of the medium. From the above formulas, the scattering cross-section C_s are proportional positive ratio to r^6, and the absorption cross-section C_a are proportional positive ratio to r^3. After we have greatly enhanced the size r of nanosilver particles, the increase of the scattering cross-section C_s is much larger than that of the absorption cross-section C_a. As a result, the enhancement of the fluorescence is greatly improved.

We discovered from the previous experiments of luminescence spectra that the visible luminescence enhancement was 1.44～2.52 times the of A/C for sample (A), which is obviously larger than that of 1.08～1.55 of B/C for sample (B). Moreover, it is fact that the infrared luminescence enhancement is 1.43～2.14 times of A/C for sample (A), which is also larger than that of 1.28～1.82 of B/C for sample (B).

From the previous experiments of fluorescence lifetime dynamics, we know that $\tau_A \approx \tau_B < \tau_C$. This means that the luminescence enhancement of sample (B) relative to sample (C) results from the Spontaneous radiation enhancement effect. Meanwhile, it also means that the luminescence enhancement of sample (A) relative to sample (B) results from the Size r effect, which is illustrated above.

3 Conclusion

It was discovered that the luminescence intensity of sample (A) is about 1.43～2.52 times larger relative to that of sample (C). Meanwhile, the luminescence intensity of sample (B) is about 1.08～1.82 times larger than that of sample (C). From the experiments of fluorescence lifetime dynamics, we know that $\tau_A \approx \tau_B < \tau_C$, which means that the luminescence enhancement of sample (B) relative to sample (C) results from the Spontaneous radiation enhancement effect. However, it also means that the luminescence enhancement of sample (A) relative to sample (B) results from the Size r effect, in which the increase of the scattering cross-section C_s is much larger than that of the absorption cross-section C_a when r is enlarged.

References

[1] Song Z F. Principle and Application of Atomic Spectroscopy and Crystal Spectroscopy. Beijing: Science Press, 1987.
[2] Yang Z, Ni W H, Yan C H, et al. J. Phys. Chem. C, 2008, 112(48): 18895.

[3] Luo Q, Chen Y R, Li Z Q, et al. Nanotechnology, 2014, 25(18): 185401.
[4] Zhan Q Q, Zhang X, He S L, et al. Laser & Photonics Rev., 2015, 9(5): 479.
[5] Cheng F R, Jing X P, Wang Z Y. Phys. Chem. Chem. Phys., 2015, 17(5): 3689.
[6] Yin Z, Xu W, Song H W, et al. Advanced Materials, 2016, 28(13): 2518.
[7] Trupke T, Shalav A, Green M A, et al. Solar Energy Materials & Solar Cells, 2006, 90(18-19): 3327.
[8] Mie G. Annalen der Physik, 1908, 25(3): 377.
[9] Mahrazl Z A S, Sahar M R, Ghoshal S K, et al. Mater. Lett., 2013, 112: 136.
[10] Reisfeld R. Lasers and Excited States of Rare-Earth, Springer-Verlag, 1977.
[11] Wu Jianghong, Cheng Peihong, Bao Jilong, et al. Spectroscopy and Spectral Analysis, 2018, 38(1): 128.
[12] Rivera V A G, Osorio S P A, Ledemi Y, et al. Opt. Express, 2010, 18(24): 25321.
[13] Fares H, Elhouichet H, Gelloz B, et al. J. Appl. Phys., 2014, 116(12): 123504.

碲化物发光玻璃中银纳米颗粒表面等离激元增强铒离子发光的研究

陈晓波[1]，李 崧[1]，赵国营[2]，龙江迷[1]，王水锋[1]，郑 东[1]，吴正龙[1]，孟少华[2]，郭敬华[1]，徐玲芝[2]，于春雷[3]，胡丽丽[3]

1. 北京师范大学应用光学北京重点实验室和物理系，北京 100875
2. 上海应用技术大学材料科学与技术系，上海 200235
3. 中国科学院上海光学精密机械研究所，上海 201800

摘 要 有趣的贵金属表面等离激元的光学性质，尤其是在发光增强领域的表现，使得它已经成为全球的一个研究热点。表面等离激元就是光与贵金属中的自由电子相互作用时，自由电子和光波电磁场由于共振频率相同而形成的一种集体振荡态。该文研究了碲化物玻璃中银纳米颗粒的表面等离激元共振增强铒离子的发光。我们测量了吸收谱、激发谱、发光谱以及荧光寿命。首先，我们挑选 365.5 和 379.0 nm 吸收峰作为激发波长测量了 385～780 nm 波长范围的可见发光光谱，发现有 4 个发光峰，依次位于 408.0，525.0，546.0 和 658.5 nm，容易指认出它们依次为铒离子的$^2H_{9/2}\rightarrow{}^4I_{15/2}$，$^2H_{11/2}\rightarrow{}^4I_{15/2}$，$^4S_{3/2}\rightarrow{}^4I_{15/2}$和$^4F_{9/2}\rightarrow{}^4I_{15/2}$的荧光跃迁；可以计算出[80 nm 平均粒径纳米银的 Er^{3+}(0.5%)Ag(0.2%)：碲化物玻璃的样品 A]的上述 4 个可见发光的峰值强度是[Er^{3+}(0.5%)：碲化物玻璃的样品 C]的大约 1.44～2.52 倍。同时，[50 nm 平均粒径纳米银的 Er^{3+}(0.5%)Ag(0.2%)：碲化物玻璃的样品 B]的上述 4 个可见发光的峰值强度是样品 C 的大约 1.08～1.55 倍。随后，我们挑选 365.5 和 379.0 nm 吸收峰作为激发波长测量了 928～1 680 nm 波长范围的近红外发光光谱，发现近红外波段有两个发光峰，位于 979.0 和 1 530.0 nm，容易指认出它们依次为铒离子的$^4I_{11/2}\rightarrow{}^4I_{15/2}$和$^4I_{13/2}\rightarrow{}^4I_{15/2}$的荧光跃迁；同样可以计算出样品 A 的上述 2 个近红外发光的峰值强度是样品 C 的大约 1.43～2.14 倍。同时，样品 B 的上述 2 个近红外发光的峰值强度是样品 C 的大约 1.28～1.82 倍。因此，发光的最大增强大约是 2.52 倍。从荧光寿命动力学实验，我们发现样品 A 的荧光寿命为 $\tau_A(550)=43.5\ \mu s$，样品 B 的荧光寿命为 $\tau_B(550)=43.2\ \mu s$，样品 C 的荧光寿命为 $\tau_C(550)=48.6\ \mu s$。这些实验结果证实了 $\tau_A\approx\tau_B<\tau_C$。它意味着样品(B)相对于样品(C)的发光增强是源于自发辐射增强效应。然而，它也意味着样品(A)相对于样品(B)的发光增强是源于纳米银颗粒的粒径尺寸 r 效应。也就是说当粒径尺寸 r 增大的时候，散射截面 C_s 和 r^6 成正比，而吸收截面 C_a 和 r^3 成正比，因此散射截面 C_s 增大的速度会远大于吸收截面 C_a 增大的速度，而散射截面 C_s 是荧光增强的原因，吸收截面 C_a 是荧光减弱的原因，所以随着银纳米颗粒尺寸的增大，其散射截面占主要部分，当发光材料和金属表面等离子体 SP 发生耦合时，能量快速的转移到金属表面等离子体 SP 上，而后被散射到远场，这有利于增强荧光。其综合的结果就导致了发光强度会随 r 的增大而增强。上述实验的结果对太阳能电池的光伏发电和生物物理应用等领域都有着很好的应用前景。

关键词 银纳米颗粒；发光增强；表面等离激元；碲化物的玻璃；铒离子

(收稿日期：2018-05-19，修订日期：2018-10-14)